

# Chloroaluminate Ionic Liquids: from their Structural Properties to their Applications in Process Intensification

B. Gilbert<sup>1</sup>, H. Olivier-Bourbigou<sup>2</sup> and F. Favre<sup>2</sup>

<sup>1</sup> Université de Liège, Laboratoire de Chimie analytique, Sart Tilman, 4000 Liège - Belgique

<sup>2</sup> Institut français du pétrole, IFP-Lyon, BP 3, 69390 Vernaison - France

e-mail: B.Gilbert@ulg.ac.be - helene.olivier-bourbigou@ifp.fr - frederic.favre@ifp.fr

**Résumé — Les liquides ioniques Chloroaluminates : De leurs propriétés structurales à leurs applications pour l'intensification des procédés** — Les propriétés structurales de nouveaux liquides ioniques organochloroaluminates, constitués à partir de mélanges de  $(\text{Ethyl})_n\text{AlCl}_{(3-n)}$  ( $n = 1$  à  $3$ ) avec du chlorure de 1-méthyl-3-butyl-imidazolium (BMIC) ont été étudiées par spectrométrie Raman. À partir de cette technique, tous les anions mono et polynucléaires ont été identifiés et quantifiés. Les mélanges mixtes formés à partir d' $\text{AlCl}_3$  et  $\text{EtAlCl}_2$  ou  $\text{EtAlCl}_2$  et  $\text{Et}_2\text{AlCl}$ , chaque couple étant à son tour mélangé avec du BMIC, ont aussi été considérés. Tous ces mélanges se comportent comme les chloroaluminates habituels : en particulier, leurs propriétés acide-base sont directement dépendantes de leurs compositions. Grâce à cette étude, il a été possible d'anticiper et d'optimiser la composition d'un liquide ionique basé sur de l' $\text{EtAlCl}_2$ , dans le but de l'utiliser pour l'oligomérisation industrielle des oléfines catalysées par les complexes du nickel, en milieux chloroaluminates. Les aspects fondamentaux de l'influence de la composition de ce solvant sur le mécanisme général de la réaction d'oligomérisation sont actuellement compris. Les liquides ioniques jouent un double rôle : ils sont à la fois solvants et activateurs du nickel (ou co-catalyseur).

**Abstract — Chloroaluminate Ionic Liquids: from their Structural Properties to their Applications in Process Intensification** — The structural properties of new organochloroaluminate ionic liquids based on mixtures of  $(\text{Ethyl})_n\text{AlCl}_{(3-n)}$  ( $n = 1$  to  $3$ ) with 1-methyl-3-butyl-imidazolium chloride (BMIC) have been studied by Raman spectroscopy. With this technique, the mono and polynuclear anions present in these melts have been identified and quantified. The mixed salts formed with  $\text{AlCl}_3$  and  $\text{EtAlCl}_2$  or  $[\text{EtAlCl}_2$  and  $\text{Et}_2\text{AlCl}]$  together with BMIC are also considered. All behave as regular chloroaluminates; in particular, their acid-base properties depend on their compositions. Thanks to this study, it has been possible to anticipate and to optimize the composition of an ionic liquid based on  $\text{EtAlCl}_2$ , with the aim of performing industrially the Ni-catalyzed olefin oligomerization in chloroaluminates. The influence of the solvent composition on the overall mechanism of the catalysis is now basically understood. The resulting ionic liquids play the dual role of solvents and nickel activator (or co-catalyst).

## INTRODUCTION

Because the constraints of environment are becoming more and more stringent, organic reactions, catalytic processes and separation technologies require the development of alternative solvents and technologies more environment-friendly.

During these last 20 years, water has emerged as a new useful reaction media [1]. But despite its “green nature”, its utilization is still limited because of the low solubility of organic hydrophobic compounds, and because water cannot be regarded as an inert solvent. More recently, other solvents such as supercritical CO<sub>2</sub> or perfluorinated solvents have proven their utility for some organic and catalytic reactions. Among them, ionic liquids are now recognized as a novel class of solvents. Since their introduction in organic synthesis more than ten years ago [2], the interest for using ionic liquids in organic catalysis has been rapidly increasing [3] and their applications range continues to expand [4]. They indeed have the advantages over conventional solvents to be liquid over a large range of temperatures and to have a non-volatile character. This latter property has probably been one of the driving forces for their development as alternative environment-friendly commonly termed “green” solvents, even if their toxicity and biodegradability are not always proven. In fact, the intense interest for these media really originates from their unique and fascinating wide range of physico-chemical properties. Their tunable polarity and hard/soft character, their negligible vapour pressure, their adjustable solvating ability make them quite different from classical organic solvents and as a consequence, the

development of novel technologies is possible. The diversity of their properties is demonstrated by their broad range of potential applications going from organic drug synthesis to high capacity batteries, novel specialty chemicals, novel materials, applications as engineering fluids, etc. [4].

They have often been used in homogeneous catalysis as an effective means for immobilization of catalysts, to solve the problem of catalyst separation and recycling. But one would expect more from ionic liquids than just the possibility of recycling the catalyst. As they impose an ionic environment, they may change the course of the reactions, and so one could expect to see a general “ionic liquid effect”.

## 1 THE EARLY DAYS OF CATALYTIC OLEFIN DIMERIZATION IN IONIC LIQUIDS

One of the first example of the use of ionic liquids as catalyst solvent is the homogeneous oligomerization of olefins catalyzed by the cationic Ni(II) organometallic complex [5-8]. This reaction is currently operated on an industrial scale (IFP-Dimersol<sup>®</sup> process) and contributes for a large part to the total volume of olefins produced by oligomerization (*Table 1*).

The IFP Dimersol<sup>®</sup> process was initiated and co-developed by Y. Chauvin at IFP in the 70th. There are two versions of this process. The «gasoline» one consists of dimerizing propene to high-octane isohexenes, especially in oil refineries that do not have petrochemicals, as in the United States. There are currently 35 plants in operation (including 18 in the

TABLE 1  
Some examples of industrial applications of homogeneous catalysis

Process	Products	Metal	Capacity (T/Year)
<b>Hydroformylation (Roelen 1938)</b>	Aldehydes, alcohols	Co, Rh	6 M
MeOH Carbonylation	<b>Acetic Acid</b>	Rh, Ir	3.5 M
<b>Polymerization (Ziegler Natta 1953)</b>	Poly Ethylene Poly Propylene Poly Butadiene, Poly Isoprene	Ti, Ni, Zr...	50 M (12.5 M of which LLDPE)
<b>Wacker Process (oxidation)</b>	Ethanal	Pd	1 M
<b>Hydrocyanation</b>	Dicyanobutane (Nylon)	Ni	200 000
Benzene Hydrogenation (IFP)	Cyclohexane (Nylon)	Ni	3 M (27 units) (first unit 1976)
<b>Olefin oligomerization/dimerization</b>			
<b>C<sub>2</sub>, C<sub>3</sub> Dimerization (IFP Dimersol E; G)</b>	C <sub>6</sub> Gasoline	Ni	<b>3 M</b> (>25 units) (first unit 1977)
<b>C<sub>4</sub> dimerization (IFP Dimersol X)</b>	mixture octenes	Ni	<b>0.2 M</b> (5 units) (first unit 1980)
<b>C<sub>2</sub> dimerization (IFP Alphabutol)</b>	1-butene LLDPE Co -monomer	Ti	<b>0.4 M</b> (20 units) (first unit 1987)
<b>C<sub>2</sub> oligomerization (IFP Alphaselect)</b>	alpha olefins (C <sub>4</sub> -C <sub>8</sub> )	Zr	commercialized
<b>C<sub>2</sub> oligo (Chevron, BP Amoco, Shell) C<sub>2</sub> trimerization (Phillips)</b>	Linear Alpha olefins 1 -hexene	Cr	<b>3.4 M</b>

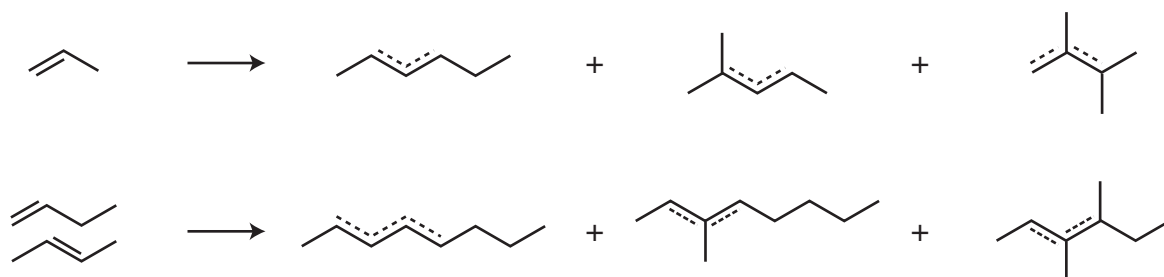


Figure 1

Dimerization of olefins: the Dimersol<sup>®</sup> process.

USA), with a combined annual output of 3.5 million tons. It was the first and only time that coordination catalysis had been used in refining. The “chemical” version of the process consists of dimerizing n-butenes to isooctenes, basic inputs for plasticizers, using the “oxo” reaction (Fig. 1).

Current production levels stand at 400 000 tons a year. This process is operated without any solvent, in the liquid phase, under mild reaction conditions. When the reaction is completed, the nickel catalyst is neutralized and the products are washed with caustic soda and water to remove the deactivated catalyst. From an industrial point of view, despite its beneficial effect on reaction velocity, the use of a solvent is not made in order to avoid any extra separation and recycling. Following his participation to a joined meeting on Molten Salts between the French and Belgian Chemical Societies in 1989, Y. Chauvin already anticipated that, considering the cationic nature of the Dimersol<sup>®</sup> nickel catalyst [9] (Fig. 2), ionic liquids based on chloroaluminate anions could be good solvents for the nickel catalyst stabilization and immobilization.

These ionic liquids indeed present several advantages for this reaction. They are non-protic solvents and therefore compatible with the metal-carbon bond and they are liquid over a large range of composition [10] (Fig. 3).

Another important motivation of performing olefin oligomerization in chloroaluminates is that oligomers and ionic liquids are very weakly miscible. The reaction system is then biphasic and the product mixture can be easily separated by decantation as a less dense second phase, without the need of adding an extractant co-solvent.

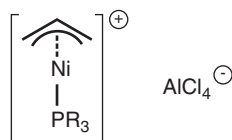


Figure 2

Cationic Ni active catalyst for olefin dimerization.

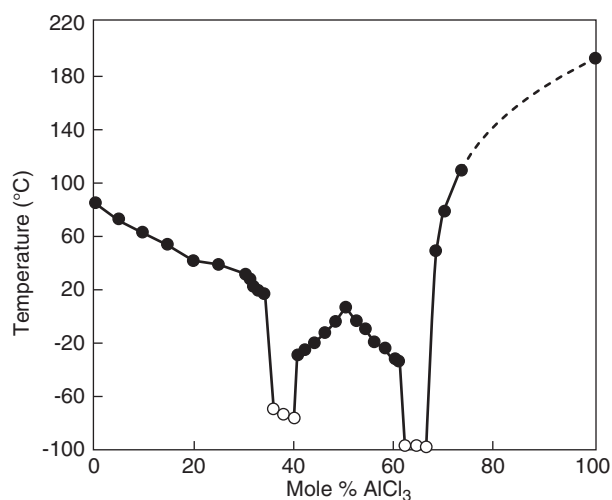


Figure 3

Phase diagram of  $\text{AlCl}_3$ /1-Ethyl-3-Methylimidazolium Chloride.

These chloroaluminates (mixtures of  $\text{AlCl}_3$  and an organic pyridinium or imidazolium chloride) were developed several years before by electrochemists who were looking for liquid electrolytes with large electrochemical windows for batteries (Fig. 4). But it was the first time that chloroaluminates were used as a combination of solvent and co-catalyst for a chemical reaction.

The challenge was to choose the right selection of both cation and anion. Besides the physico-chemical properties described above, the chemical composition proved to be of utmost importance. The first observation was that the oligomerization reaction did not occur in *basic* chloroaluminates. These ionic liquids indeed contain an excess of coordinating chloride anions that inhibit the Ni catalyst activity by forming stable blue tetrahedral  $[\text{NiCl}_4]^{2-}$  anions. On the other hand, acidic chloroaluminates seemed particularly suitable. For practical reasons, it is necessary to generate the active Ni catalyst “*in situ*” in the ionic liquid starting from an air stable commercial Ni(II) salt. This is the reason why the attention

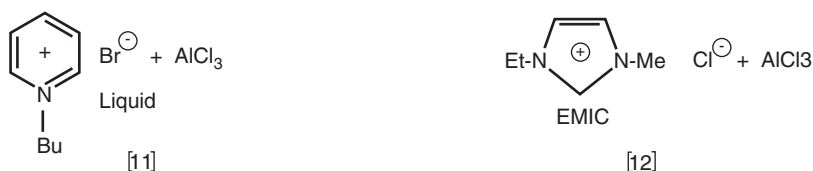


Figure 4

The first development of halogenoaluminate ionic liquids.

was focused to the organochloroaluminates based on the mixture of ethyl aluminium dichloride (EADC) and 1-Methyl-3-Butylimidazolium Chloride (BMIC).

However, at that time, these ionic liquids were new and their acid-base properties, so important for the catalytic processes, were not known. Since these depend directly on the structural properties, a new research was initiated to try to determine the species formed in such mixtures as a function of the compositions and then to deduce the acid-base equilibria involved. The major investigations were made on these systems by Raman spectroscopy at the University of Liège and the most important results are summarized in the next section.

## 2 RAMAN SPECTROSCOPY OF ROOM-TEMPERATURE ORGANOCHLOROALUMINATE IONIC LIQUIDS APPLICABLE TO THE DIFASOL PROCESS

The Raman spectra of mixtures made of  $(\text{Ethyl})_n\text{AlCl}_{(3-n)}$  ( $n = 0$  to 3) mixed with BMIC were studied as a function of their composition. The mixed salts formed with  $\text{Al}_2\text{Cl}_6$  and  $\text{EtAlCl}_2$  or  $[\text{EtAlCl}_2$  and  $\text{Et}_2\text{AlCl}]$  are also considered.

When a pyridinium or imidazolium chloride is mixed with  $\text{AlCl}_3$ , it has been shown that the well-known  $\text{AlCl}_4^-$  and  $\text{Al}_2\text{Cl}_7^-$  anions are formed in equilibrium and their relative proportion depends on the melt composition [11-12]. The Raman spectra of such mixtures are quite difficult to obtain because of fluorescence originating from organic impurities. However, by improving the purification of the starting materials, it is now possible to record good quality spectra on such systems. Figure 5 shows the Raman spectrum of  $\text{Al}_2\text{Cl}_7^-$  which has never been published in detail.

In this spectrum, eleven bands (noted by a capital letter) can be assigned to  $\text{Al}_2\text{Cl}_7^-$ , the others belonging either to the organic cation or to some  $\text{AlCl}_4^-$ . Because only six bands are expected for a linear molecule (of  $D_{3d}$  symmetry), this result confirms that the anion must be bent, as already suggested [13]. However, a non-linear molecule (symmetry  $C_s$ ) is expected to present 21 Raman active modes and ten lines are then too weak or hidden by others. This emphasizes the difficulty of deducing symmetry for a molecule simply by counting the number of experimental bands with their polarization state.

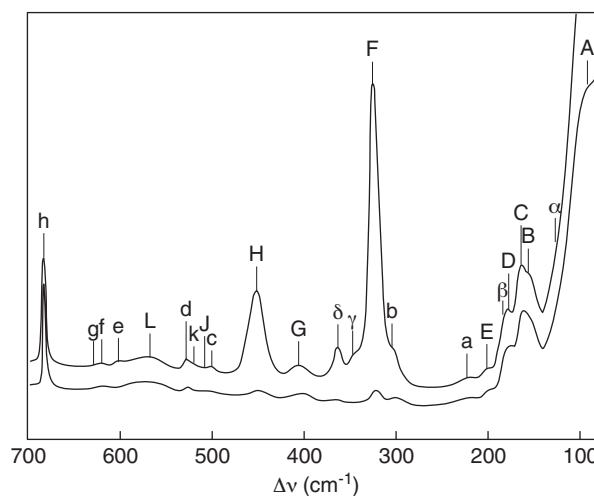


Figure 5

Raman spectrum of the  $\text{Al}_2\text{Cl}_7^-$  anion; capital letters:  $\text{Al}_2\text{Cl}_7^-$ ; lowercase letters: organic cation (butyl pyridinium); greek letters:  $\text{AlCl}_4^-$  and  $\text{Al}_3\text{Cl}_{10}^-$ .

During our study of  $\text{EtAlCl}_2$ -BMIC mixtures, we have shown that another technique can be applied to deduce the stoichiometry of species in equilibrium [14]. It involves the quantitative measurement of the intensity ratios of two bands, each characteristic of one species, as a function of the mixture composition. In the present case, this ratio has been measured for the  $349\text{ cm}^{-1}$  band of  $\text{AlCl}_4^-$  and the  $307\text{ cm}^{-1}$  band of  $\text{Al}_2\text{Cl}_7^-$  at various melt compositions (Fig. 6). If the model is correct, this ratio should be proportional to the ratio of the amounts of concerned species:

$$R = \frac{I_{307}}{I_{349}} = K \frac{[\text{Al}_2\text{Cl}_7^-]}{[\text{AlCl}_4^-]}$$

The ratios  $[\text{Al}_2\text{Cl}_7^-]/[\text{AlCl}_4^-]$  are readily calculated from the assumed stoichiometry and mass balance consideration. Figure 7 shows a plot of the measured intensity ratios versus the respective calculated concentration ratios. A straight line is observed indicating that the model is indeed correct. In addition, the slope of that line represents the ratio of the

scattering efficiencies of the species of concern. Here, the experimental ratio is  $0.87 \pm 0.02$ , which means that the main vibration of  $\text{Al}_2\text{Cl}_7^-$  scatters less per mole than the corresponding one of  $\text{AlCl}_4^-$ .

In the case of  $\text{EtAlCl}_2$ -BMIC mixtures, a straight line was also observed in similar conditions, indicating that the reaction  $\text{EtAlCl}_3^- + \text{EtAlCl}_2 \rightarrow \text{Et}_2\text{AlCl}_5^-$  is quantitative, at least up to a composition of 0.66 (expressed in mole fraction  $N$ ) [14]. It should be noted that this latter result and the aluminium electronegativity measurements [15] do not agree with the work of Keller *et al.* [16] where it is proposed that  $\text{EtAlCl}_2$  dimer exists as major species even in a 1:1 melt. From our measurements, a

1:1 or a more basic mixture never showed any of the very characteristic  $(\text{EtAlCl}_2)_2$  bands. Indeed Figure 8 shows that these two spectra are clearly distinct.

Because of their possible interest in the two-phase catalysis, the  $\text{Et}_2\text{AlCl}$ -BMIC and  $\text{Et}_3\text{Al}$ -BMIC mixtures which are also liquid at room temperature have been investigated as well. The spectra of 1:1 mixtures were found totally different than the ones of the corresponding pure ethylaluminium compound (Figs. 8-10). In addition, if the amount of BMIC is further increased, the main spectrum stays unchanged, only the intensity of the  $[\text{BMI}]^+$  cation bands increases. We have then assumed that the  $\text{AlCl}_4^-$  equivalent species are formed,

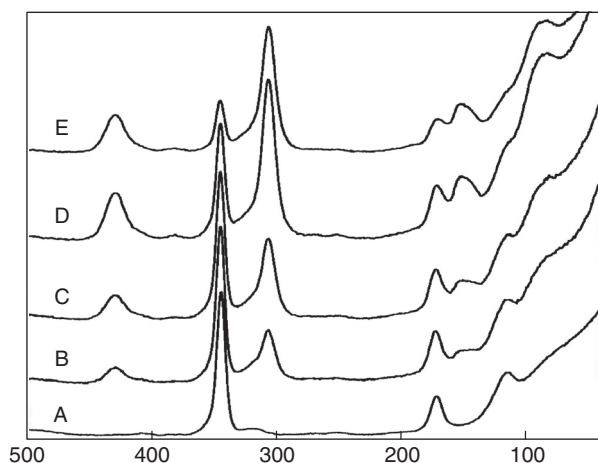


Figure 6

Raman spectra of  $\text{AlCl}_3$ -BMIC mixtures at various compositions.  $N = 0.475$  (A); 0.56 (B); 0.582 (C); 0.617 (D); 0.639 (E) respectively.  $N =$  molar fraction of  $\text{AlCl}_3$ .

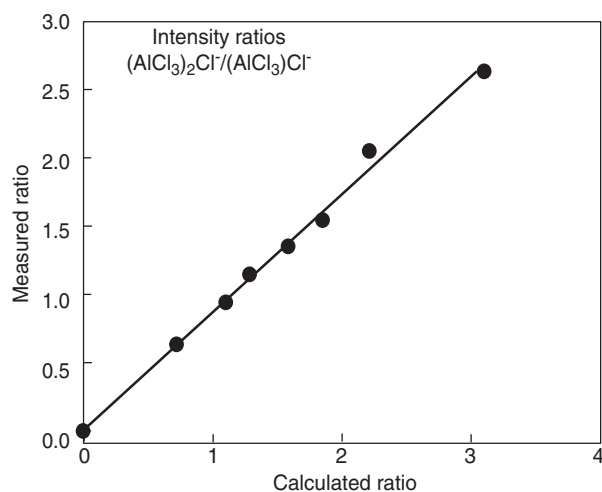


Figure 7

Plot of the  $I_{307}/I_{349}$  ratio as a function of the  $\text{Al}_2\text{Cl}_7^-/\text{AlCl}_4^-$  calculated ratio.

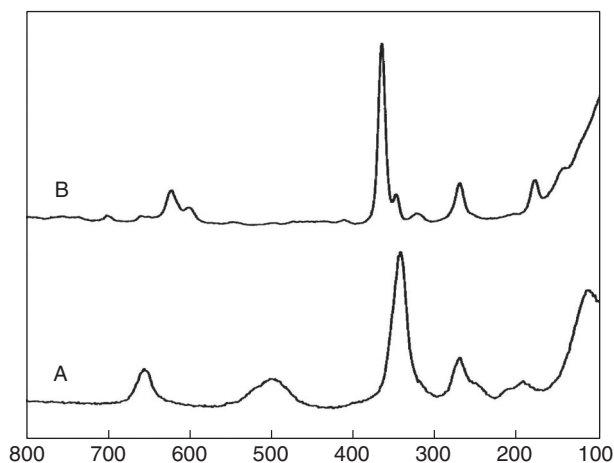


Figure 8

Raman spectra of: (A) pure  $\text{EtAlCl}_2$ ; (B)  $\text{EtAlCl}_2$ -BMIC 1:1 mixture.

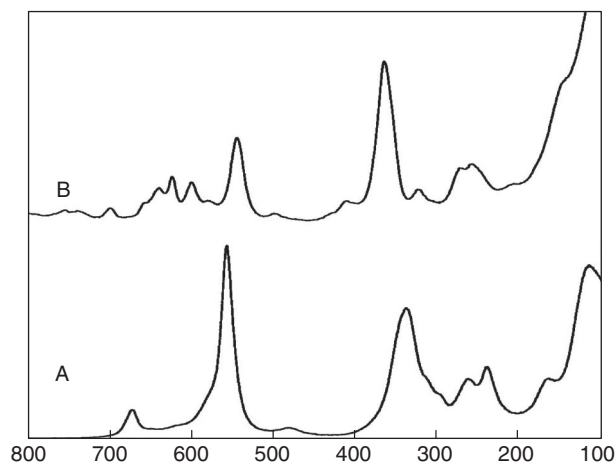


Figure 9

Raman spectra of: (A) pure  $\text{Et}_2\text{AlCl}$ ; (B)  $\text{Et}_2\text{AlCl}$ -BMIC 1:1 mixture.

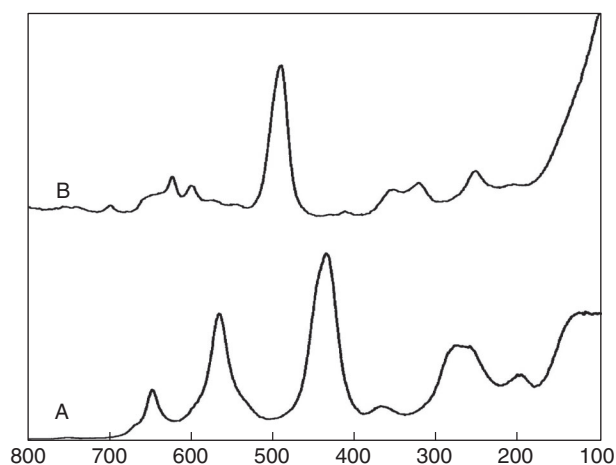


Figure 10

Raman spectra of: (A) pure  $(\text{Et}_3\text{Al})_2$ ; (B)  $\text{Et}_3\text{Al}$ -BMIC 1:1 mixture.

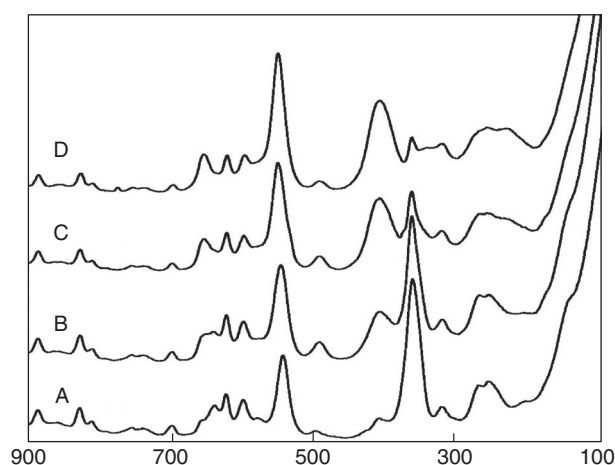


Figure 11

Raman spectra of  $\text{Et}_2\text{AlCl}$ -BMIC mixtures at various compositions,  $N = 0.495$  (A);  $0.572$  (B);  $0.631$  (C);  $0.675$  (D) respectively.

*i.e.*  $\text{Et}_2\text{AlCl}_2^-$  and  $\text{Et}_3\text{AlCl}^-$  respectively. These species are characterized by their main band at  $366$  and  $492$   $\text{cm}^{-1}$  respectively.

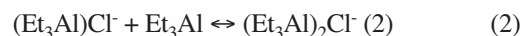
When  $\text{Et}_2\text{AlCl}$  is added to a 1:1  $\text{Et}_2\text{AlCl}$ -BMIC mixture, the bands assigned to  $\text{Et}_2\text{AlCl}_2^-$  are progressively replaced by another distinct spectrum which is not the one of  $\text{Et}_2\text{AlCl}$  (Fig. 11). By analogy to the behaviour of the other above systems, this new species has been assumed as  $(\text{Et}_2\text{AlCl})_2\text{Cl}^-$ ; it exhibits one major band at  $410$   $\text{cm}^{-1}$  and a weaker one at  $366$ . In this case, the  $366$   $\text{cm}^{-1}$  band of  $(\text{Et}_2\text{AlCl})_2\text{Cl}^-$  overlaps with the intense band of  $\text{Et}_2\text{AlCl}_2^-$ . However, because the spectrum of  $\text{Et}_2\text{AlCl}_2^-$  can be obtained alone, it can be easily quantitatively subtracted from each spectrum of Figure 11. The intensity ratio of all the resulting spectrum stays constant at any composition up to  $N = 0.67$ , a proof of the existence of only one additional species.

The same quantitative procedure described above for  $\text{Al}_2\text{Cl}_7^-$  has then been applied to the intensity ratios of the  $410$   $\text{cm}^{-1}$  band of the hypothetical  $(\text{Et}_2\text{AlCl})_2\text{Cl}^-$  over the  $366$   $\text{cm}^{-1}$  band of  $\text{Et}_2\text{AlCl}_2^-$ . A straight line is obtained between these ratios and the calculated amounts of species showing that the following reaction should occur (Equation 1):



Upon addition of  $\text{Et}_3\text{Al}$  to a 1:1  $\text{Et}_3\text{Al}$ -BMIC mixture, the shape of the  $\text{Et}_3\text{AlCl}^-$  spectrum does not change very much except that the main  $493$   $\text{cm}^{-1}$  band intensity seems to increase. In order to solve this problem, we have added to each investigated mixture an internal intensity standard. This standard must be miscible, inert and should not exhibit any band in the region of interest. We then chose to refer all intensity measurements to the intensity of the  $992$   $\text{cm}^{-1}$  band

of  $\text{C}_6\text{H}_6$  whose concentration was kept constant in each mixture. Examples of such spectra are shown in Figure 12 where it can be seen that the  $493$   $\text{cm}^{-1}$  band intensity increases regularly with the  $\text{Et}_3\text{Al}$  addition. We then proposed that this band is made of two components: one is the  $\text{Et}_3\text{AlCl}^-$  which decreases progressively and is replaced by the bridged  $(\text{Et}_3\text{Al})_2\text{Cl}^-$ . Again, the intensity ratios of the two components, obtained by computer, were found directly proportional to the expected amounts calculated from the reaction (Equation 2):



The above considerations are valid for compositions up to  $N = 0.66$ . Above  $0.66$ , it has been shown that the  $\text{AlCl}_3$  based mixtures contain, in addition to the  $\text{AlCl}_4^-$  and  $\text{Al}_2\text{Cl}_7^-$ , the  $\text{Al}_3\text{Cl}_{10}^-$  trimer. The composition range where the mixture stays liquid is however very limited [17-19]. In the  $\text{EtAlCl}_2$ -BMIC mixtures, trimers are also formed but they are rapidly replaced by  $(\text{EtAlCl}_2)_2$  which is miscible all the way up to pure  $(\text{EtAlCl}_2)_2$  [14]. For the  $\text{Et}_2\text{AlCl}$ -BMIC and  $\text{Et}_3\text{Al}$ -BMIC mixtures where  $N > 0.66$ , the spectra can be interpreted respectively as mixtures of  $(\text{Et}_2\text{AlCl})_2\text{Cl}^-$  or  $(\text{Et}_3\text{Al})_2\text{Cl}^-$  with  $(\text{Et}_2\text{AlCl})_2$  or  $(\text{Et}_3\text{Al})_2$ . No trimer was found and demixion occurs at  $N = 0.8$  ( $\text{Et}_2\text{AlCl}$ ) or  $N = 0.75$  ( $\text{Et}_3\text{Al}$ ). The demixed phase is made of the corresponding pure ethylaluminium.

All these experiments have allowed measurement of the scattering efficiencies within each couple  $(\text{Ethyl})_n\text{AlCl}_{(3-n)}\text{Cl}^- - ((\text{Ethyl})_n\text{AlCl}_{(3-n)})_2\text{Cl}^-$  ( $n = 0$  to  $3$ ). In order to determine the concentration of any such species involved in a reaction, it is necessary to measure the scattering efficiencies of the various couples versus each other. To this end, we have prepared mixed salts formed from  $\text{Al}_2\text{Cl}_6$

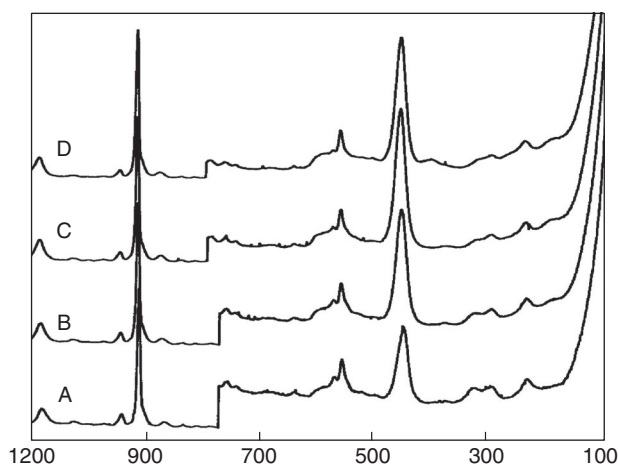


Figure 12

Raman spectra of  $\text{Et}_3\text{Al}$ -BMIC mixtures with  $\text{C}_6\text{H}_6$  as internal intensity standard:  $N = 0.5$  (A); 0.588 (B); 0.649 (C); 0.708 (D). From  $800\text{ cm}^{-1}$ , the sensitivity is reduced 5 times.

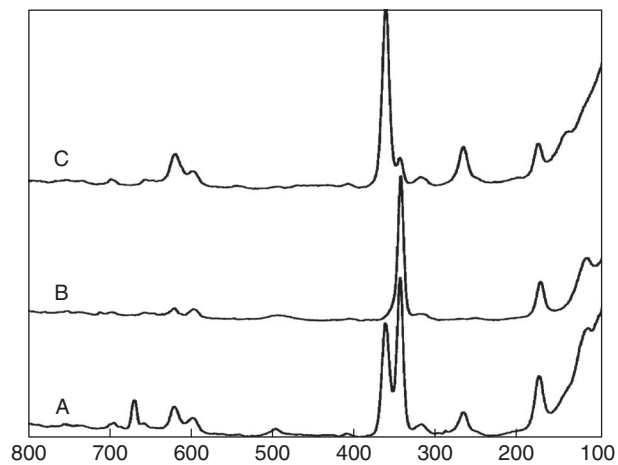


Figure 13

Raman spectra of: (A)  $\text{AlCl}_3$ - $\text{EtAlCl}_2$ -BMIC 0.5:0.5:1; (B)  $\text{EtAlCl}_2$ -BMIC 1:1; (C)  $\text{AlCl}_3$ -BMIC 1:1.

and  $(\text{EtAlCl}_2)_2$  or  $(\text{EtAlCl}_2)_2$  and  $(\text{Et}_2\text{AlCl})_2$ . Figure 13 shows the spectrum obtained by mixing a 0.5:0.5:1  $\text{AlCl}_3$ - $\text{EtAlCl}_2$ -BMIC mixture (spectrum A, Fig. 13). This spectrum exhibits only the characteristic bands of  $\text{AlCl}_4^-$  and  $\text{EtAlCl}_3^-$  and no other species is observed. Consequently, the number of mole of each species must be the same and the ratio of scattering coefficients is simply the ratio of the heights of the respective  $\nu_1$  major bands. A similar experiment has been made with a 0.5:0.5:1  $\text{EtAlCl}_2$ - $\text{Et}_2\text{AlCl}$ -BMIC mixture to measure the relative scattering coefficients between  $\text{EtAlCl}_3^-$  and  $\text{Et}_2\text{AlCl}_2^-$ . Finally, all the scattering coefficients have been expressed versus a common reference, the  $\nu_1$   $\text{AlCl}_4^-$  band.

To complete this study, we have recorded the spectra of mixed acidic systems. First, an equimolar  $\text{EtAlCl}_2$  and  $\text{Et}_2\text{AlCl}$  mixture of global Lewis acid composition  $N = 0.66$  exhibits a spectrum of its own (characterized by a main band at  $366\text{ cm}^{-1}$ , Fig. 14A) which corresponds most probably to the mixed dimer  $(\text{EtAlCl}_2)(\text{Et}_2\text{AlCl})\text{Cl}^-$ . Although this spectrum resembles that of  $\text{Et}_2\text{AlCl}_2^-$ , the confusion is not possible because several strong bands are present which do not belong to any known species up to now. Secondly, the equivalent mixture made from  $\text{AlCl}_3$  and  $\text{EtAlCl}_2$  is more complex (Fig. 14B). One can indeed recognize the main bands of  $\text{Al}_2\text{Cl}_7^-$  ( $307\text{ cm}^{-1}$ ) and that of  $(\text{EtAlCl}_2)_2^-$  ( $349\text{ cm}^{-1}$ ). By subtracting these two spectra from the original, a third spectrum is left which belongs to the mixed dimer  $(\text{AlCl}_3)(\text{EtAlCl}_2)\text{Cl}^-$  (main band at  $333\text{ cm}^{-1}$ ). Hence, this dimer is not totally stable and dissociates through the following reaction (Equation 3):



which also means that the association of  $\text{EtAlCl}_2$  with  $\text{AlCl}_3$  is not as strong as the one with  $\text{Et}_2\text{AlCl}$ .

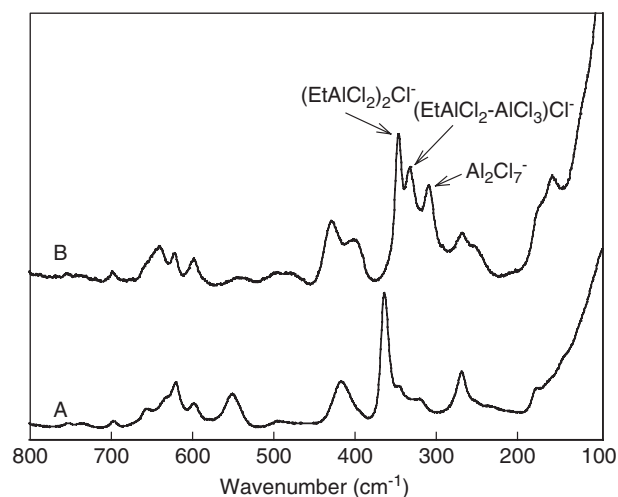


Figure 14

Raman spectra of: (A)  $\text{EtAlCl}_2$ - $\text{Et}_2\text{AlCl}$ -BMIC 1:1:1 mixture; (B)  $\text{AlCl}_3$ - $\text{EtAlCl}_2$ -BMIC 1:1:1 mixture.

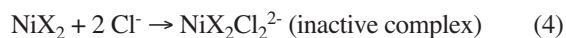
As conclusion of this preliminary study, we have shown that organochloroaluminate salts based on mixtures of  $(\text{Ethyl})_n\text{AlCl}_{(3-n)}$  ( $n = 1$  to 3) with 1-methyl-3-butylimidazolium chloride (BMIC) are liquid near room temperature in a very large composition range. The structural properties of all these mixtures have been studied by Raman spectroscopy and compared with the ones of classical chloroaluminate melts [10]. As in the latter case, they form mono and polynuclear anions and a whole new family of species has been identified. It was also found that the tendency to polymerize decreases with the increase of ethyl

groups number. The ethylaluminium derivatives mixed with an organic chloride thus form a new class of ionic mixtures with a behaviour very similar to the one of regular chloroaluminates. Similar acid-base concepts should then apply and are function of the composition: mixtures of EtAlCl<sub>2</sub>-BMIC, Et<sub>2</sub>AlCl-BMIC and Et<sub>3</sub>Al-BMIC all behave as basic or acidic Lewis mixtures when the molar ratios are respectively below or higher than one. Mixed mixtures lead to similar conclusions. All the identified species have been collected in Table 2 as a function of the composition.

Because of the complexity of the spectra, the existence and the stoichiometry of the various species have been confirmed by a quantitative study of the bands intensity variation as a function of the composition. A consequence of this study is that it is now possible to identify and quantify by Raman spectroscopy any of the reaction products involved in an industrial process based on these melts. Because of the overlap of some of the major bands, this identification and quantification can be made safely by considering the full spectrum of one given species and not the main bands only. This feature will be fully emphasized in the next section.

Regarding the industrial application aiming to perform olefin oligomerization in chloroaluminates containing EtAlCl<sub>2</sub>, the influence of the solvent composition on the overall mechanism of the catalysis is now basically understood: the resulting ionic liquids play the dual role of solvents and nickel activator (or co-catalyst) (Equations 4, 5).

*in basic chloroaluminates*



*in acidic alkylchloroaluminates*



### 3 QUANTITATIVE STUDY BY RAMAN SPECTROSCOPY OF THE STABILITY OF ORGANOCHLOROALUMINATES IONIC LIQUIDS IN PRESENCE OF AN ALIPHATIC HYDROCARBON PHASE

As said above, one of the major applications of acidic alkylchloroaluminates ((BMIC)-EthylAlCl<sub>2</sub>) is their use as solvent for catalytic reactions such as the dimerization of olefins catalyzed by nickel complexes (the Difasol® process) [5-8]. These ionic liquids indeed proved to be particularly effective for a two-phase catalysis process since the products are not soluble in the molten phase and they can be extracted by an aliphatic hydrocarbon phase.

However, the main difficulty is to suppress or limit catalyst leaching in the organic phase and to avoid the loss of the ethylaluminium necessary for the alkylation and activation of the nickel catalyst precursor. In a previous work, we have shown that, during the extraction process, it is possible to analyse separately and in situ, both the organic and molten salt phases by Raman spectroscopy. It was found that due to the total miscibility of the chloroethylaluminium compounds and hydrocarbons, disproportionation occurs when a molten salt based on dialkylimidazolium chloride and alkylaluminium chloride is contacted with an hydrocarbon phase [20]. Depending on the extracted ethylaluminium nature, the resulting composition of the molten salt phase is expected to change and consequently will affect the catalysis results.

It has also been shown that, for a same global aluminium molar fraction, the global acidity level of BMIC-[EtAlCl<sub>2</sub>+AlCl<sub>3</sub>] mixture was higher than that of BMIC-EtAlCl<sub>2</sub> mixture [15]. Since the activity of the nickel system is dependent upon this Lewis acidity, ionic liquids based on the mixtures of EtAlCl<sub>2</sub>+AlCl<sub>3</sub> are preferable. An accurate

TABLE 2

Anionic species identified from the Raman spectra as a function of the molar fraction of (EthyI)<sub>n</sub>AlCl<sub>(3-n)</sub>

EADC = EtAlCl<sub>2</sub>; DEAC = Et<sub>2</sub>AlCl; TEA = Et<sub>3</sub>Al

<i>n</i> = 0	Cl <sup>-</sup> AlCl <sub>4</sub> <sup>-</sup>	AlCl <sub>4</sub> <sup>-</sup> Al <sub>2</sub> Cl <sub>7</sub> <sup>-</sup>	Al <sub>2</sub> Cl <sub>7</sub> <sup>-</sup> Al <sub>3</sub> Cl <sub>10</sub> <sup>-</sup>		<i>MIXED SPECIES</i>  (AlCl <sub>3</sub> )(EADC)Cl <sup>-</sup>  (EADC)(DEAC)Cl <sup>-</sup>  (EADC)(DEAC)
<i>n</i> = 1	Cl <sup>-</sup> (EADC)Cl <sup>-</sup>	(EADC)Cl <sup>-</sup> (EADC) <sub>2</sub> Cl <sup>-</sup>	(EADC) <sub>2</sub> Cl <sup>-</sup> (EADC) <sub>3</sub> Cl <sup>-</sup>	(EADC) <sub>3</sub> Cl <sup>-</sup>	
<i>n</i> = 2	Cl <sup>-</sup> (DEAC)Cl <sup>-</sup>	(DEAC)Cl <sup>-</sup> (DEAC) <sub>2</sub> Cl <sup>-</sup>	(DEAC) <sub>2</sub> Cl <sup>-</sup> DEAC	(DEAC) <sub>2</sub> Cl <sup>-</sup> DEAC	
<i>n</i> = 3	Cl <sup>-</sup> (TEA)Cl <sup>-</sup>	(TEA)Cl <sup>-</sup> (TEA) <sub>2</sub> Cl <sup>-</sup>	(TEA) <sub>2</sub> Cl <sup>-</sup> TEA		
0	0.50	0.67	0.75	1	

Mole fraction of (EthyI)<sub>n</sub>AlCl<sub>(3-n)</sub> (*n* = 0 to 3).

adjustment of the  $\text{EtAlCl}_2$  to  $\text{AlCl}_3$  ratio is thus required to optimize the efficiency of the catalytic system.

In our initial extraction measurements, the molten salts were made of single mixtures of dialkylimidazolium chloride and monoalkylaluminium chloride ( $\text{EtAlCl}_2$ ) without adding  $\text{AlCl}_3$  [14]. Upon addition of  $\text{AlCl}_3$  to the alkylchloroaluminate, the resulting mixed ionic liquid exhibits a more complex structural behaviour than single mixtures since mixed anionic species are formed (see below). The purpose of this section is to present a thorough quantitative investigation of the behaviour of the mixed molten salt phase as well as of the organic phase by Raman spectroscopy, upon extraction by an aliphatic hydrocarbon phase.

Since the industrial melts exhibit a strong fluorescence, only the FT-Raman instrument leads to meaningful spectra on such samples. On the other hand, it is important to evaluate quantitatively the proportion of the various components especially in the molten phase. Considering the different intensity response of the FT-Raman versus our classical Raman instruments, all our previous measurements were remade and the relative scattering coefficients measured again with the FT instrument.

Although, as we were showing above, the structure of  $\text{BMIC-AlCl}_3$  and  $\text{BMIC-EtAlCl}_2$  mixtures is well known, involving equilibria respectively between  $\text{AlCl}_4^-$ - $\text{Al}_2\text{Cl}_7^-$  and  $\text{EtAlCl}_3^-$ - $(\text{EtAlCl}_2)_2\text{Cl}^-$ , new Raman spectra confirm that the  $\text{BMIC-AlCl}_3$ - $\text{EtAlCl}_2$  mixtures exhibit an additional mixed  $(\text{EtAlCl}_2\text{-AlCl}_3)\text{Cl}^-$  species which seems to play an important role in the catalytic process.

On the other hand, the spectra recorded from various mixtures  $\text{BMIC-AlCl}_3$ - $\text{EtAlCl}_2$  1/1/ $X$  where  $X$  varied from 0.1 to 1, show that the amount of the mixed  $(\text{EtAlCl}_2\text{-AlCl}_3)\text{Cl}^-$  species, characterized by its major band at  $333\text{ cm}^{-1}$ , is proportional to the added  $\text{EtAlCl}_2$ .

Dynamic extractions of the molten phase by an aliphatic hydrocarbon (cyclopentane) have been performed by using the same apparatus as we have described previously [20]. By shifting vertically the laser beam, it allows to record, as a function of time, Raman spectra of all phases, the molten salt which is stirred and the leaching organic phase which is refreshed continuously. The choice of cyclopentane is based on two reasons: first, it exhibits only relatively weak Raman bands in the spectrum range of interest and this may be important since we wish to detect low amount of extracted product; secondly, its spectrum contains a line at  $711\text{ cm}^{-1}$  which can serve as internal standard of intensity. This band however was soon realized as not belonging to cyclopentane itself but to 2-2-dimethylbutane present as impurity. Since it is difficult to remove this impurity by simple distillation and since the location and intensity of the  $711\text{ cm}^{-1}$  band is ideal as reference, we choose to use the same large batch of cyclopentane contaminated by a small amount of dimethylbutane thorough all the measurements. The intensity

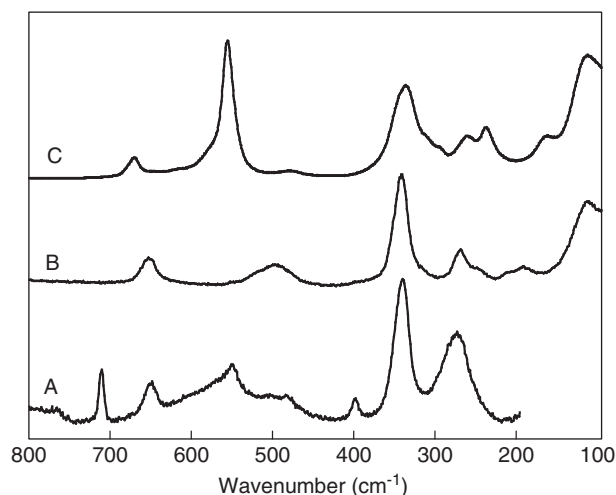
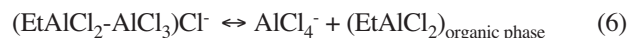


Figure 15

Raman spectra of: (A) the organic phase after extraction from a 1/1/1  $\text{BMIC-AlCl}_3$ - $\text{EtAlCl}_2$  melt; (B) pure EADC; (C) pure DEAC.

ratio of the  $711\text{ cm}^{-1}$  band reference band was checked periodically versus the intensity of the main  $886\text{ cm}^{-1}$  line of the cyclopentane to make sure it stays constant. Hence, the mixture cyclopentane-dimethylbutane will be referred below as “cyclopentane solvent”.

Dynamic extraction measurements by cyclopentane have then been made first from a  $\text{BMIC-AlCl}_3$ - $\text{EtAlCl}_2$  1/1/1 until there is no more change in the spectra of each phase (about 48 hours). Besides the bands of the cyclopentane solvent, the spectrum of the organic phase after extraction is characteristic at first sight of  $\text{EtAlCl}_2$  only (Figs. 15A, B). Considering that  $\text{AlCl}_4^-$  stays in the molten phase, the proposed reaction is then as follows (Equation 6):

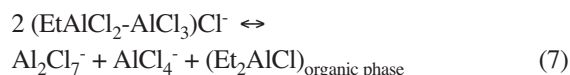


The melt loses its  $\text{EtAlCl}_2$  and becomes progressively less acidic explaining why, in principle, at some point of the industrial process, the catalysis will stop functioning, unless  $\text{EtAlCl}_2$  is continuously supplied.

From calibration curves realized in cyclopentane and from the measurement of the  $\text{EtAlCl}_2$  main band intensity referred to the intensity of the  $711\text{ cm}^{-1}$  line of cyclopentane solvent, the quantity of extracted  $\text{EtAlCl}_2$  in the organic phase can be measured and compared with the initial content of the melt. In the present case, only 70% is found in the organic phase and the resulting melt should then correspond to a 1/1/0.3 melt. The resulting spectrum of the melt after extraction and the spectrum of a synthetic  $[\text{BMIC-AlCl}_3\text{-EADC}]$  1/1/0.3 melt have then been compared (Fig. 16). Clearly, both spectra do not match exactly. If  $\text{AlCl}_4^-$  is indeed the main component in

both spectra, the spectrum of the melt after extraction (Fig. 16A) contains much more  $\text{Al}_2\text{Cl}_7^-$  than the other (Fig. 16B).

The reason for the disagreement is that during the extraction process of a mixed mixture, only  $\text{EtAlCl}_2$  has been considered up to now. Figure 15 shows that  $\text{Et}_2\text{AlCl}$  (DEAC) which can be identified by its band at  $558\text{ cm}^{-1}$  must actually be also taken into account; its contribution is low but not negligible. Indeed, the production of DEAC can originate from a disproportionation of the molten phase (Equation 7):



Considering that:

- in the spectrum of Figure 16A (the ionic phase), the contribution of an ethylaluminium is very low which means that all the ethylaluminium species have been extracted;
- the non-found 30% of  $\text{EtAlCl}_2$  (initially present in the melt as  $(\text{EtAlCl}_2\text{-AlCl}_3)\text{Cl}^-$ ) has disproportionated into equal amounts of  $\text{Al}_2\text{Cl}_7^-$ ,  $\text{AlCl}_4^-$  and  $\text{Et}_2\text{AlCl}$  (which has left the molten salt phase), the final total composition of the molten phase should correspond to a mixture containing 85% of  $\text{AlCl}_4^-$  and 15% of  $\text{Al}_2\text{Cl}_7^-$  or a mixture  $\text{BMIC-AlCl}_3$  1/1.15. This time, the Raman spectrum of a synthesized close to 1/1.15 mixture (Fig. 16C) matches very well the spectrum of Figure 16A.

In order to understand the conditions affecting the nature of the extracted ethylaluminium, measurements have been performed on a large number of  $\text{BMIC-xAlCl}_3\text{-yEtAlCl}_2$

compositions where  $x$  and (or)  $y$  varied while keeping the sum  $(x + y)$  such as the melt stays always acidic. In all these experiments, the molten mixture of the required composition is made first and stirred to ensure full homogeneity, then it is added to the extraction cell and the extraction experiment is started.

Table 3 presents the extraction results when the molten phase is a mixture of  $\text{BMIC-AlCl}_3$  of fixed composition (equimolar mixture) to which  $\text{EtAlCl}_2$  has been progressively added. For low initial  $\text{EtAlCl}_2$  content in the melt, only  $\text{EtAlCl}_2$  is found in the organic phase after extraction. When the amount of  $\text{EtAlCl}_2$  reaches a certain level,  $\text{Et}_2\text{AlCl}$  starts to be extracted in addition to  $\text{EtAlCl}_2$  and must be accounted to evaluate the total amount of  $\text{EtAlCl}_2$  consumed during the extraction process. By comparison with the melt content, it is also found that the amount of  $\text{EtAlCl}_2$  consumed by extraction is directly proportional to the mixed  $(\text{EtAlCl}_2\text{-AlCl}_3)\text{Cl}^-$  anion content. Lowering the loss of  $\text{EtAlCl}_2$  in the industrial process can then be achieved by using melts of low  $\text{EtAlCl}_2$  content.

Table 4 presents the effect of varying the  $\text{AlCl}_3$  content while the initial content of  $\text{EtAlCl}_2$  is maintained constant. The results clearly indicate that the less acidic the melt is (the Lewis acidity level is here fixed by  $\text{AlCl}_3$  which is a stronger acid than  $\text{EtAlCl}_2$ ), the more the equilibrium is shifted to the extraction of  $\text{Et}_2\text{AlCl}$  instead of  $\text{EtAlCl}_2$ . This result is also in agreement with our previous findings where the extracted product from a melt  $\text{BMIC-EtAlCl}_2$  (thus containing no  $\text{AlCl}_3$ ) is only  $\text{Et}_2\text{AlCl}$  [20]. It is finally interesting to note that in the compositions range of Table 4, the total amount of  $\text{EtAlCl}_2$  consumed is constant.

Finally, Table 5 shows the extraction results from melts where the total amounts of  $\text{AlCl}_3$  plus  $\text{EtAlCl}_2$  are constant. It emphasizes again the influence of the acidity level of the initial melt on the results. Despite a constant amount of acidic species, the extracted product nature varies which means that the acidity level of the melt is not constant and confirms that  $\text{AlCl}_3$  is a stronger acid than  $\text{EtAlCl}_2$ . In addition, the maximal extraction occurs from melts where the  $\text{AlCl}_3$  and  $\text{EtAlCl}_2$  contents are similar.

The present results show that the dynamic extraction process is more complicated than initially thought [20]. In the case of the mixed mixtures  $\text{BMIC-AlCl}_3\text{-EtAlCl}_2$ , two extraction reactions must indeed be taken into account simultaneously, leading to the formation of  $\text{EtAlCl}_2$  and  $\text{Et}_2\text{AlCl}$ . The extent of each reaction was found to be melt composition dependent: the proportion of  $\text{EtAlCl}_2$  versus  $\text{Et}_2\text{AlCl}$  increases with the acidity level of the initial melt, mainly determined by its  $\text{AlCl}_3$  content, the strongest Lewis acid of the family.

This problem has been overlooked before and one of the consequences is that the consumption of  $\text{EtAlCl}_2$  by extraction cannot be calculated by measuring only the  $\text{EtAlCl}_2$  content in the organic phase. It can be calculated either from the final composition of the molten phase or from the total amount of  $\text{EtAlCl}_2$  and  $\text{Et}_2\text{AlCl}$  in the organic phase. Since the extraction process mechanism is now fully understood,

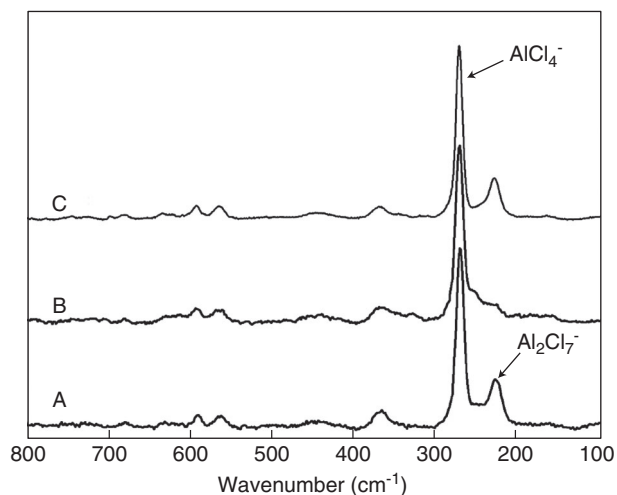


Figure 16

Raman spectra of (A) the resulting melt after extraction of a 1/1/1  $\text{BMIC-AlCl}_3\text{-EtAlCl}_2$  mixture by cyclopentane; (B) a synthetic melt 1/1/1.03  $\text{BMIC-AlCl}_3\text{-EtAlCl}_2$ ; (C) a synthetic melt 1/1.18  $\text{BMIC-AlCl}_3$ .

TABLE 3  
Extraction results from a BMIC-AlCl<sub>3</sub>-EtAlCl<sub>2</sub> 1/1/*X* (*X* variable)

Initial composition <i>X</i> = variable	Extracted EADC (%) DEAC Extraction neglected	Final Composition Composition DEAC extraction neglected	<i>Ri</i> (DEAC/CYCLO) *	Total EADC consumed (%) DEAC extraction included	Final Composition DEAC extraction included
1/1/0.20	-	1/1/0.20	-	-	1/1/0.20
1/1/0.30	30 ± 2	1/1/0.21	-	30 ± 2	1/1/0.21
1/1/0.40	40 ± 2	1/1/0.24	-	40 ± 2	1/1/0.24
1/1/0.50	45 ± 2	1/1/0.27	0.23	58 ± 2	1/1.06/0.21
1/1/0.75	55 ± 2	1/1/0.34	0.37	77 ± 2	1/1.11/0.17
1/1/1.0	70 ± 2	1/1/0.30	0.50	100 ± 2	1/1.15

\*  $Ri_{(DEAC/CYCLO)}$  = Intensity ratio of the 550 cm<sup>-1</sup> (DEAC) over the reference line of cyclopentane solvent at 711 cm<sup>-1</sup>.

TABLE 4  
Extraction results from a BMIC-AlCl<sub>3</sub>-EtAlCl<sub>2</sub> 1/*Y*/0.5 (*Y* variable)

Initial Composition <i>Y</i> = variable	$\chi$ (EADC) *	$\chi$ (AlCl <sub>3</sub> ) **	<i>Ri</i> (DEAC/CYCLO) ***	Total EADC consumed (%) extraction DEAC included	Final Composition extraction DEAC Included
1/1/0.5	0.20	0.40	0.23	58 ± 2	1/1.06/0.21
1/1.22/0.5	0.18	0.45	0.14	61 ± 2	1/1.26/0.19
1/1.5/0.5	0.17	0.50	-	60 ± 2	1/1.50/0.20

\*  $\chi$  (EADC) = mole fraction of EADC, (= *n* EADC / (*n* BMIC + *n* AlCl<sub>3</sub> + *n* EADC));

\*\*  $\chi$  (AlCl<sub>3</sub>) = mole fraction of AlCl<sub>3</sub>, (= *n* AlCl<sub>3</sub> / (*n* BMIC + *n* AlCl<sub>3</sub> + *n* EADC));

\*\*\*  $Ri_{(DEAC/CYCLO)}$ : as in Table 3.

TABLE 5  
Extraction results from a BMIC-AlCl<sub>3</sub>-EtAlCl<sub>2</sub> 1/*Y*/*X* (*X* + *Y* = constant)

Initial Composition <i>X</i> + <i>Y</i> = 1.5	$\chi$ (EADC) *	$\chi$ (AlCl <sub>3</sub> ) **	Extracted EADC (%)	Final Composition DEAC extraction neglected	Total EADC consumed (%) DEAC extraction Included
1/1/0.5	0.20	0.40	45 ± 2	1/1/0.27	58 ± 2
1/0.75/0.75	0.30	0.30	12 ± 2	1/0.75/0.66	100 ± 2
1/0.5/1	0.40	0.20	7 ± 2	1/0.50/0.93	100 ± 2
1/0.2/1.3	0.52	0.08	4 ± 2	1/0.2/1.25	66 ± 2

\*  $\chi$  (EADC): as in Table 4

\*\*  $\chi$  (AlCl<sub>3</sub>): as in Table 4.

conclusions could be drawn to propose a melt composition exhibiting the lowest loss in ethylaluminium while keeping the acidity level compatible with the catalysis process.

#### 4 THE BIPHASIC DIFASOL PROCESS

As explained above, in order to maintain a high Lewis acidity, a good candidate for the biphasic oligomerization catalysis is an ionic liquid involving contents in EtAlCl<sub>2</sub> and

AlCl<sub>3</sub> respectively low and high. This ionic liquid could be prepared from commercially available *N,N'*-dialkylimidazolium chloride. Its synthesis has already been validated on several tens of kilograms using IFP-Lyon pilot plant facilities and is ready for an industrial application. Laboratory experiments [7] were performed with a Ni(II) salt and the BMIC-AlCl<sub>3</sub>-EtAlCl<sub>2</sub> ionic liquid in semi-batch way to evaluate the activity and the selectivity of the system in dimers. In order to demonstrate the recyclability of the catalyst, a continuous flow pilot plant was operated. This

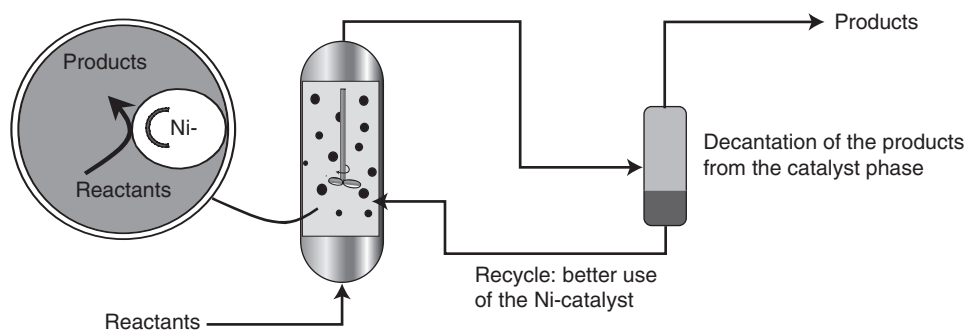


Figure 17

Biphasic octene dimerization.

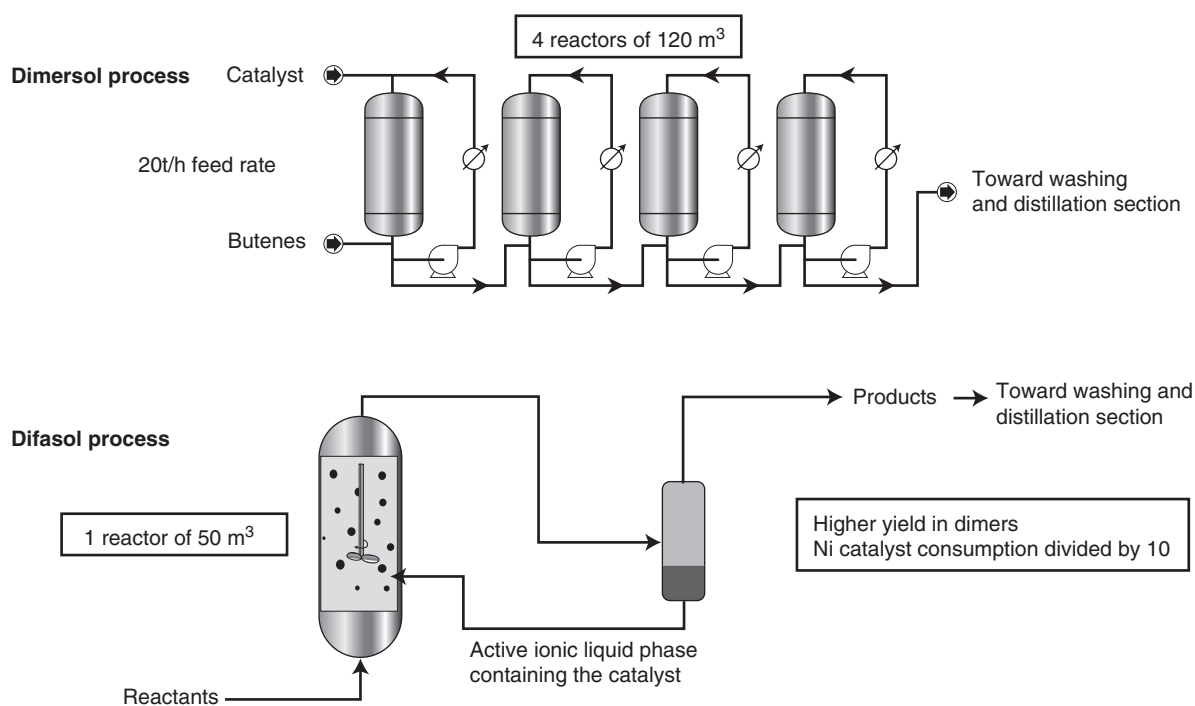


Figure 18

Toward process intensification by using catalytic biphasic system in ionic liquids.

continuous test was run with a representative industrial  $C_4$  raffinate II cut composed of 70% butenes (27% of which is 1-butene) and 1.5% isobutene (the remaining being n-butane and isobutane) which is introduced continuously in the well-stirred reactor. The reactor is operated full of liquid. The effluent (a mixture of the two liquid phases) leaves the reactor via an overflow and is transferred to a phase separator. The separation of the ionic liquid (density around 1200 g/L) and the oligomers occurs rapidly and completely (favoured by the difference in densities). The ionic liquid and the catalyst are recycled to the reactor. The test was conducted over a period of

5500 hours after which it was deliberately stopped. No ionic liquid can be detected in the products. After the 5500 hour continuous run, the volume of the ionic liquid phase was the same as that at the start. Throughout the whole test, the butene conversion is maintained above 70%. Butenes are converted into octenes with high selectivity (95% of octenes relative to the total products). In such system, consecutive side reactions (octenes + butenes) are minimized due to the lower solubility of octenes compared to butenes in the ionic liquid (Fig. 17).

The octene distribution is similar to that produced by the conventional homogeneous industrial Dimersol process. The

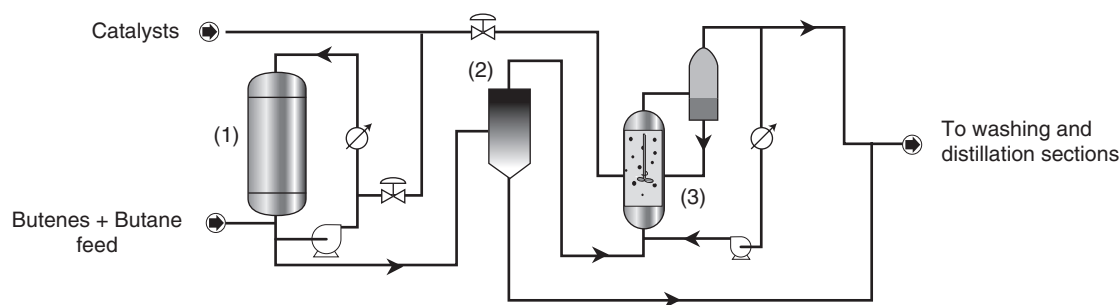


Figure 19

Dimersol + Difasol package reaction. (1) Dimersol reactor; (2) Vaporization-condensation; (3) Difasol reactor.

reaction products form a second liquid phase which can be separated from the ionic liquid by simple decantation. Diethylaluminum dichloride has to be injected continuously or batchwise in order to maintain the reaction performances. The reaction productivity expressed in kg of dimers produced per gram of nickel is much higher than that obtained in classical organic solvents. Despite the utmost importance of physical limitations such as solubility and mixing efficiency of two-phase systems, an apparent reaction rate constant of one relative to the olefin monomer has been determined in a batch-wise experiment. Extrapolation of the process to the industrial scale leads to the following advantages over the existing homogeneous Dimersol process:

- the system can be run with alkene poor feeds (as low as 20% butene) and hence streams such as raffinate II (27% 1-butene, 44% other butenes, 29% butanes) are suitable feeds;
- lower catalyst consumption, especially the nickel component, which implies lower catalyst cost and less disposal problems;
- higher dimer selectivity. The overall yield of  $C_8$  octenes from the process can be 15% higher than in the homogeneous process;
- a much smaller reactor (*Fig. 18*) can give the same throughput to  $C_8$  alkenes.

This results in an overall improvement of the economy of the process.

Difasol can also be ideally suited for use after a first homogeneous dimerization step. This first homogeneous step offers the possibility to purify the feed, in a very efficient way, from trace impurities. A package is proposed consisting of a first homogeneous dimerization step, which acts mainly as a pretreatment of the feedstock, and a biphasic section. This arrangement ensures an overall more efficient catalyst utilization and a significant increase in the yield of octenes (*Fig. 19*). As an example, dimer selectivity in the range 90–92% with butene conversion in the range 80–85% can be obtained (*Table 6*).

TABLE 6  
Comparison of the operating parameters for a homogeneous (Dimersol) butene dimerisation plant with a hybrid plant in which 50% conversion is received in a Dimersol plant, but the product is fed to a Difasol plant [8]

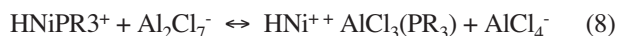
Factor	Dimersol	Dimersol + Difasol
Octene yield/%	68	75
Conversion/%	80	81
Selectivity/%	85	92
Nickel consumption	100 <sup>a</sup>	70
Aluminium consumption	100 <sup>a</sup>	Much reduced
Relative chemical consumption <sup>b</sup>	100 <sup>a</sup>	82
Relative CAPEX <sup>b</sup>	1.5	1.3
Relative OPEX <sup>b</sup>	1.5	1.2

<sup>a</sup> Base case; <sup>b</sup> Per ton of octenes produced.

## 5 EXTENSION OF THE APPLICATION OF THE BIPHASIC DIFASOL PROCESS

Propene dimerization can also be performed using the same ionic liquid based catalytic system. When using a nickel salt precursor without any special ligand, hexene dimers are obtained without any regio-selectivity (typically a mixture of dimethylbutenes, methylpentenes, hexenes) (*Fig. 1*). The addition of bulky basic phosphines such as triisopropylphosphine can drive the reaction to high selectivity in 2,3-dimethylbutenes (1-DMB and 2-DMB). 2,3-dimethylbutenes are highly valuable products used as starting material for the synthesis of fine chemicals. This phosphine effect, well-known in homogeneous systems, can be maintained in acidic chloroaluminates providing a proper adjustment of the ionic liquid acidity. However, the 2,3-dimethylbutene selectivity decreases very rapidly if no additional phosphine is added. This has been ascribed to the existence of a competition for the basic phosphine between the soft active

nickel species and the hard aluminium chloride Lewis acid potentially present in the solvent according to the following Equation 8:



In order to maintain the 2,3-dimethylbutene selectivity, organic bases were added to the ionic liquid to buffer its Lewis acidity. Aromatic hydrocarbons proved to be the most suitable bases as they do not interfere with the active nickel while preventing the  $\text{PR}_3/\text{AlCl}_3$  interaction thus maintaining the 2,3-dimethylbutene selectivity high.

Thanks to the biphasic technique, the dimerization can also be extended to less reactive longer chain olefins ( $\text{C}_5$  feed) allowing the production of decenes and nonenes through co-dimerization of butenes and pentenes.

## CONCLUSION

This work is an example of a fundamental study performed on new solvents which has led to a practical industrial application: the dimerization of olefins through a biphasic catalysis process, the Difasol process. The solvent is an ionic liquid based on mixtures of  $(\text{Ethyl})_n\text{AlCl}_{(3-n)}$  ( $n = 1$  to 3) with 1-butyl-3-methyl-imidazolium chloride (BMIC). At first, Raman spectroscopy has allowed identification and quantification of the main anionic species constituting the liquid and consequently the acid-base properties. In general, it was found that these mixtures behave similarly as regular chloroaluminates in the sense that the acidity (expressed here in terms of chloroacidity) is very much affected by the composition, especially around the equimolar composition: for an excess of  $(\text{Ethyl})_n\text{AlCl}_{(3-n)}$ , the mixtures are acidic and then suitable for a process involving acid catalysis. The resulting ionic liquids play the dual role of solvent and nickel catalyst activator.

Next, since an aliphatic hydrocarbon, insoluble to the ionic phase, is used to collect the reaction products, Raman spectroscopy was also used to investigate the stability of the ionic phase during the extraction process. It was indeed found that, during extraction, some  $\text{EtAlCl}_2$  is lost but the mechanism of this loss is complex: a disproportionation occurs, depending on the initial acidity and affecting the composition of the resulting ionic liquid. From dynamic compositional measurements of all liquid phases (ionic and extracting aliphatic phases), conclusions could be drawn on the extraction mechanism. The best solvent is a mixed acidic  $\text{BMIC}-[\text{EtAlCl}_2+\text{AlCl}_3]$  mixture where the  $\text{EtAlCl}_2$  is low; this mixture retains the high acidity level necessary for the catalysis together with the lowest loss rate of  $\text{EtAlCl}_2$ .

Finally, the developed mixture has been tested in a pilot plant facility and put to work for 5500 hours. This process showed several advantages over the classical ones. Among them, the butene conversion throughout the whole test was

maintained above 70%. The reaction productivity expressed in kg of dimers produced per gram of nickel is much higher than that obtained in classical organic solvents. The overall Ni-catalyst consumption can be decreased. The total volume of the reaction section is much smaller than in the homogeneous process. These results should lead to an overall improvement of the economy of the Difasol process and to possible extensions.

## ACKNOWLEDGMENTS

The authors wish to express their warm thanks to Y. Chauvin who, not only has initiated this work, but has always been the driving force for its completion. We wish to acknowledge his participation and assistance, together with his kindness in any circumstances, his sustained enthusiasm and inventiveness during the work. B. Gilbert has particularly appreciated his unreservedly welcome. The authors also thank all the PhD students who have participated in this work, J.P. Pauly and S. Dechamps for the Raman experiments, I. Guibard, F. Di Marco-Van Tiggelen and S. Einloft. Finally, the IFP is acknowledged for continuous financial support.

## REFERENCES

- Cornils B., Herrmann W.A. (2005) Aqueous-Phase Catalysis, in *Multiphase Homogeneous Catalysis*, Cornils B., Herrmann W.A., Horvath I.T., Leitner W., Mecking S., Olivier-Bourbigou H., Vogt D. (eds.), Wiley-VCH, Weinheim.
- Chauvin Y., Olivier-Bourbigou H. (1995) *Chemtech*, **9**, 25, 26.
- Olivier-Bourbigou H., Magna L. (2002) *J. Mol. Catal.* **182-183**, 419.
- Zhang Z. (2006) *Adv. Catal.*, 153-237; Weyershausen B., Lehmann K. (2005) *Green Chem.* **7**, 15; Taubert A., Li Z. (2006) *Dalton Trans.*, 723; Zhao H., Xia S., Ma P. (2005) *J. Chem. Technol. Biot.* **80**, 10, 1089; Freemantle M. (2007) *C&EN* **85**, 01, 23; Short P.L. (2006) *C&EN* **84**, 17, 15.
- Chauvin Y., Gilbert B., Guibard I. (1990) *J. Chem. Soc. Chem. Commun.*, 1715.
- Olivier H., Chauvin Y., Hirschauer A. (1992) *A.C.S. Meeting*, San Francisco, April 5-10, Division of Petroleum Chemistry, Preprint Vol. 37, No. 3, pp. 780-785.
- Chauvin Y., Einloft S., Olivier H. (1995) *Ind. Eng. Chem. Res.* **34**, 4, 1149.
- Favre F., Forestière A., Hugues F., Olivier-Bourbigou H., Chodorge J.A. (2005) *Oil Gas-Eur. Mag.* **2**, 83.
- Wilke G., Bogdanovic B., Hardt P., Heimbach O., Kroner W., Oberkirch W. (1966) *Angew. Chem. Int. Edit. Engl.* **5**, 151.
- Hussey C.L. (1983) *Advances in Molten Salt Chemistry*, Mamantov G. (ed.), Elsevier, Vol. 5, p. 185.
- Gale R.J., Gilbert B., Osteryoung R.A. (1978) *Inorg. Chem.* **17**, 2728.

- 12 Wilkes J.S., Levisky J.A., Wilson R.A., Hussey C.L. (1982) *Inorg. Chem.* **21**, 1263.
- 13 Gale R.J., Osteryoung R.A. (1980) *Inorg. Chem.* **19**, 2240.
- 14 Gilbert B., Chauvin Y., Guibard I. (1991) *Vib. Spectrosc.* **1**, 299.
- 15 Chauvin Y., Di Marco-Van Tiggelen F., Olivier H. (1993) *J. Chem. Soc. Dalton Trans.*, 1009.
- 16 Keller C.E., Carper W.R., Piersma B.J. (1993) *Inorg. Chim. Acta* **209**, 239.
- 17 Torsi G., Mamantov G., Begun G.M. (1970) *Inorg. Nucl. Chem. Lett.* **6**, 553.
- 18 Dymek C.J. Jr, Wilkes J.S., Einarsrud M.A., Øye H.A. (1988) *Polyhedron* **7**, 1139.
- 19 Abdul-Sada A.K., Greenway A.M., Seddon K.R., Welton T. (1989) *Org. Mass Spectrometry* **24**, 917.
- 20 Gilbert B., Chauvin Y., Olivier H., Di Marco F. (1995) *J. Chem. Soc. Dalton Trans.*, 3867.

*Final manuscript received in April 2007*

Copyright © 2007 Institut français du pétrole

Permission to make digital or hard copies of part or all of this work for personal or classroom use is granted without fee provided that copies are not made or distributed for profit or commercial advantage and that copies bear this notice and the full citation on the first page. Copyrights for components of this work owned by others than IFP must be honored. Abstracting with credit is permitted. To copy otherwise, to republish, to post on servers, or to redistribute to lists, requires prior specific permission and/or a fee: Request permission from Documentation, Institut français du pétrole, fax. +33 1 47 52 70 78, or [revueogst@ifp.fr](mailto:revueogst@ifp.fr).